

## Supplemental Figure Legends:

**Supplementary Figure 1. Smart-Seq2 Dataset Metrics and Cell Type Marker Expression - Related to Figure 1.** (A) Density plot of total mRNAs per cell after Monocle relative2abs transformation. (B) Tables of number of cells per plate (top), number of cells at each developmental age (middle), and QC metrics of the entire Smart-Seq2 dataset. (C) Graph of the number of genes expressed per cell, faceted by developmental age. (D) Dispersion plot of the high variance genes (red) used for dimension reduction. Black line indicates gam fit. E) tSNE dimension reduction with cells colored by the plate that they came from. F-I) Cellular heatmaps of reduced tSNE maps for (F) markers of proliferative RPCs (*Ccnd1*, *Cdk4*, *Dkk3*, *Pax6*), (G) markers of the G1/S phases of the cell cycle (*Ccne2* and *Pcna*) or G2/M (*Ccnb1* and *Ube2c*), (H) markers of neurogenic progenitors (*Atoh7*, *Neurod1*, *Neurog2*, and *Olig2*), or (I) cell type-specific markers including those of photoreceptors (*Crx*), retinal ganglion cells (*Isl1* and *Pou4f2*) and amacrine cells (*Tfap2b*).

**Supplementary Figure 2. 10x Dataset Metrics- Related to Figure 1.** (A) Number of replicate datasets and total number of single cells profiled corresponding to each developmental age. (B) Breakdown of QC metrics according to the individual samples, including number of cells, mean reads per cell, and total number of sequencing reads of each library. (C) QC metrics of the unique molecular identifiers (UMI) and Genes detected across all the cells. (D-E) Boxplots of the total mRNAs or UMIs detected per cell faceted by (D) developmental age or (E) sample. (F-I) UMAP dimension reduction of the 10x dataset with cells colored by (F) developmental age, (G) the original cell type annotation based on clustering from individual ages, (H) cluster designation following Mclust analysis, (I) or re-annotation of Mclust clusters in UMAP space. Re-annotation of cell type was based on expression of known marker genes of retinal cell types within each cluster. (J) Graph displaying the proportion of retinal cell type profiled at each developmental age. (K) Graph displaying the proportion of each developmental age that each retinal cell type was captured. (L) Graph displaying the proportion of mature retinal cell types captured at each developmental age with RPCs and neurogenic cells eliminated from the analysis. (M) Graph displaying the proportion of RPC, neurogenic and gliogenic (or mature Müller glia) cells capture at each developmental age.

**Supplementary Figure 3. Dispersion plots indicating data fit and high variance genes- Related to Figure 1.** (A) Dispersion plots displaying high variance genes (black) across all cells profiled from individual ages. (B-C) Dispersion plots of high variance genes across aggregated cells across the (B) entire dataset and used for UMAP dimension reduction, or (C) annotated retinal cells and used for developmental order in pseudotime analysis across the retinal cells.

**Supplementary Figure 4. tSNE plots of 10x Samples by developmental age - Related to Figure 1.** tSNE dimension reduction of 10x datasets across all cells at (A) E11, (C) E12, (E) E14, (G) E16, (I) E18, (K) P0, (M) P2, (O) P5, (Q) P8, (S) P14 and annotated retinal cells at (B) E11, (D) E12, (F) E14, (H) E16, (J) E18, (L) P0, (N) P2, (P) P5, (R) P8, (T) P14. Cells are colored by annotated cell type after clustering performed

on tSNE plots of individual samples. Cell types were re-annotated after samples were subset to retinal cells only and recursive tSNE dimension reduction was performed on a new set of high variance genes within the retinal cells.

**Supplementary Figure 5. Amacrine and horizontal cell trajectory - Related to Figures 1 and 2.** (A-B) UMAP dimension reductions of the full retina dataset showing transcript expression of (A) the horizontal cell-specific *Lhx1* transcript and (B) the horizontal cell-promoting transcription factor *Prox1* within cells contained within the amacrine cell trajectory. *Prox1* expression is also observed within RPCs, neurogenic cells, bipolar cells and amacrine cells, similar to previous reports {Dyer, 2003 #5284}. Cellular expression is colored on a scale of low (grey) to high (red) expression. (C) LargeVis dimension reduction on the subset of cells from UMAP representations annotate as amacrine cells. Colors represent re-annotation of cell types based on known marker gene expression within clusters of cells. (D) UMAP representation indicating the position of the starburst amacrine cells and horizontal cells within the full retina dataset. Starburst amacrine cells are classified as amacrine cells within Figure 1G and subsequent analyses on the full dataset. (E) Complex pseudotime tree on the amacrine cell trajectory with cells colored by annotated cell type from the largeVis dimension reduction. (F) Examples of gene expression across pseudotime of transcripts that display differential expression across the annotated amacrine, horizontal and starburst amacrine cells. Transcript expression within aggregated cell types across pseudotime is represented by the alternately colored lines. Abbreviations: Photo. Precurs. – Photoreceptor Precursors; RGCs – Retinal Ganglion Cells.

**Supplementary Figure 6. Complex pseudotime trees of annotated cell features - Related to Figure 2.** (A) Cell type proportions of the subset of ~32,000 cells used as input for pseudotime analyses. (B-C) Comparisons of (B) the proportions of cell types and (C) proportions cells of given developmental ages between the full dataset (Full) and the cells used as input for pseudotime analyses (Subset). (D-F) Complex pseudotime trees resulting from pseudotime analysis on ~32,000 retinal cells colored by (D) Pseudotime value, (E) developmental age, and (F) annotated cell type. (F) Complex pseudotime trees are faceted to show cells with individual cell type annotations.

**Supplementary Figure 7. BEAM analysis – bipolar and photoreceptor cells versus amacrine/horizontal cells - Related to Figure 2.** Heatmap of transcripts that display state-dependent differential expression between the bipolar and photoreceptor cell branch (red in complex pseudotime tree) and the amacrine/horizontal cell branch. Heatmaps represent gene expression across pseudotime starting from the top of the complex pseudotime tree (center of heatmaps) and progressing through the pseudotime tree towards the cell types of interest (periphery of heatmaps). All genes displayed significant differential expression ( $q < 1.0e-20$ ) by the BEAM test.

**Supplementary Figure 8. BEAM analysis – bipolar cells versus photoreceptor cells - Related to Figure 2.** Heatmap of transcripts that display state-dependent differential expression between the bipolar (red in complex pseudotime tree) and the photoreceptor cell branch (blue in complex pseudotime tree). Heatmaps represent gene

expression across pseudotime starting from the top of the complex pseudotime tree (center of heatmaps) and progressing through the pseudotime tree towards the cell types of interest (periphery of heatmaps). All genes displayed significant differential expression ( $q < 1.0e-20$ ) by the BEAM test.

**Supplementary Figure 9. BEAM analysis – late cells versus early cells - Related to Figure 2.** Heatmap of transcripts that display state-dependent differential expression between the late cell types (red in complex pseudotime tree) and the early cell types (RGCs and early RPCs; blue in complex pseudotime tree). Heatmaps represent gene expression across pseudotime starting from the top of the complex pseudotime tree (center of heatmaps) and progressing through the pseudotime tree towards the cell types of interest (periphery of heatmaps). All genes displayed significant differential expression ( $q < 1.0e-20$ ) by the BEAM test.

**Supplementary Figure 10. BEAM analysis – RGCs versus early RPCs - Related to Figure 2.** Heatmap of transcripts that display state-dependent differential expression between the RGCs (red in complex pseudotime tree) and the Early RPCs (blue in complex pseudotime tree). Heatmaps represent gene expression across pseudotime starting from the top of the complex pseudotime tree (center of heatmaps) and progressing through the pseudotime tree towards the cell types of interest (periphery of heatmaps). All genes displayed significant differential expression ( $q < 1.0e-20$ ) by the BEAM test.

**Supplementary Figure 11. BEAM analysis – Late RPCs and Müller glia versus amacrine/horizontal, bipolar and photoreceptor cells - Related to Figure 2.** Heatmap of transcripts that display state-dependent differential expression between the late RPCs and Müller glia (red in complex pseudotime tree) and the amacrine/horizontal cells, bipolar cells and photoreceptors (blue in complex pseudotime tree). Heatmaps represent gene expression across pseudotime starting from the top of the complex pseudotime tree (center of heatmaps) and progressing through the pseudotime tree towards the cell types of interest (periphery of heatmaps). All genes displayed significant differential expression ( $q < 1.0e-20$ ) by the BEAM test.

**Supplementary Figure 12. BEAM analysis – Late RPCs versus Müller glia - Related to Figure 2.** Heatmap of transcripts that display state-dependent differential expression between the late RPCs (red in complex pseudotime tree) and the Müller Glia (blue in complex pseudotime tree). Heatmaps represent gene expression across pseudotime starting from the top of the complex pseudotime tree (center of heatmaps) and progressing through the pseudotime tree towards the cell types of interest (periphery of heatmaps). All genes displayed significant differential expression ( $q < 1.0e-20$ ) by the BEAM test.

**Supplementary Figure 13. BEAM analysis on amacrine Cell trajectory pseudotime analysis – starburst amacrine versus other amacrine cells - Related to Figure 2.** Heatmap of transcripts that display state-dependent differential expression between the Starburst amacrine cells (red in complex pseudotime tree) and other amacrine cells

(blue in complex pseudotime tree). Heatmaps represent gene expression across pseudotime starting from the top of the complex pseudotime tree (center of heatmaps) and progressing through the pseudotime tree towards the cell types of interest (periphery of heatmaps). All genes displayed significant differential expression ( $q < 1.0e-20$ ) by the BEAM test.

**Supplementary Figure 14. BEAM analysis on amacrine cell trajectory pseudotime analysis – horizontal cells versus amacrine cells - Related to Figure 2.** Heatmap of transcripts that display state-dependent differential expression between the horizontal cells (red in complex pseudotime tree) and amacrine cells (blue in complex pseudotime tree). Heatmaps represent gene expression across pseudotime starting from the top of the complex pseudotime tree (center of heatmaps) and progressing through the pseudotime tree towards the cell types of interest (periphery of heatmaps). All genes displayed significant differential expression ( $q < 1.0e-20$ ) by the BEAM test.

**Supplementary Figure 15. Primary RPC and neurogenic RPC cell pseudotime - Related to Figure 3.** (A) Heatmap of the normalized expression of 40 core Notch-pathway genes, as identified from MSigDB, across pseudotime. Cells were grouped into 11 groups encompassing the entire range of the RPC pseudotemporal analysis from early pseudotime (top rows of heatmap) through late pseudotime (bottom rows of heatmap) (B) Heatmap of differentially expressed genes across pseudotime of the subset of RPCs and grouped by developmental age. (C) Results of EVA analysis displaying relative dissimilarity of the Fgf- (top), Notch- (middle), and Wnt-signaling pathways within RPCs from E11 to P5. (D) Graph of the proportions of cells arising from various developmental ages across the RPC, Neurogenic Cell, and Müller glial cell pseudotime analysis. (E) Pseudotime density plot of cells in the RPC, Neurogenic Cell, and Müller glial cell pseudotime analysis colored by developmental age, showing three relative clusters corresponding to early neuroepithelial cells, early RPCs and neurogenic cells, and late RPCs, late neurogenic cells and Müller glial cells. (F) Graph depicting the proportions of cells at individual developing ages in the RPC, Neurogenic Cell, and Müller glial cell pseudotime analysis that are annotated as individual cell types. \*\*\* indicates  $p < 0.001$  from EVA analysis; ns – not significant

**Supplementary Figure 16. scCoGAPS pattern weights within complex pseudotime plots of retinal cells - Related to Figure 4.** Complex pseudotime trees displaying pattern weight of individual cells within pseudotime on the subset of ~32,000 retinal cells. Individual cell pattern weights are plotted for each cell, with corresponding values progressing from low pattern weight (grey) to high pattern weight (blue).

**Supplementary Figure 17. NFI transcription factors expression within the developing retina - Related to Figure 5.** (A) Developmental time-series of *in situ* hybridization showing expression of *Nfia*, *Nfib*, and *Nfix* within the developing retina. UMAP dimension reduction plots displaying expression of (B) *Nfia*, (C) *Nfib*, and (D) *Nfix* within the full retina scRNA-seq dataset, displaying high-levels of expression of the NFI transcription factors within late RPCs. Cellular expression is colored on a scale of low (grey) to high (red) expression.

**Supplementary Figure 18. Immunohistochemistry of cell type markers within NFI transcription factor conditional knockout retinas - Related to Figure 5.**

Immunohistochemistry performed on P14 retinas examining changes in marker gene protein expression across control or *Chx10:Cre-GFP* mediated conditional knockouts of *Nfia*, *Nfib*, *Nfix*, *Nfia/b*, or *Nfia/b/x*. *Chx10:Cre-GFP* transgene is shown in green, with nuclei counterstained in merged images. (A) Immunohistochemistry for NFI protein expression shows efficiency of NFI transcription factor knockout. (B-D) Retinal progenitor cell markers (B) *Lhx2*, (C) *Pax6* and (D) *Vsx2* are not up-regulated with the maintenance of RPC proliferation in *Nfia/b* and *Nfia/b/x* conditional knockouts. (B) *Lhx2*-positive Müller glia are lost in *Nfia/b* and *Nfia/b/x* conditional knockouts. (C) Amacrine cell marker *Pax6* is maintained (D) A significant fraction of *Vsx2*-positive bipolar cells are lost in *Nfia/b/x* triple mutants. (E) Expression of *Brn3*-positive retinal ganglion cells. (F) Expression of Calbindin-positive horizontal cells. (G) Expression of *Tfap2a*-positive amacrine cells. (H) Most of the *Isl1*-positive bipolar cells are lost in *Nfia/b/x* triple conditional mutant retinas. (I) Expression of Recoverin-positive photoreceptors. (J) Both *Nfia/b* and *Nfia/b/x* conditional mutants show a large loss of P27Kip-positive Müller glial cells. Asterisk indicate regions in which cell type markers are lost. Arrowheads indicate remaining sparse labeling of cell type markers. Scale bars - 100µm

**Supplementary Figure 19. Conditional knockout of NFI transcription factors results in loss of retinal architecture, glial activation and maintenance of RPC proliferation - Related to Figure 6.**

(A) Immunohistochemistry on P14 retinas for glial fibrillary activating protein (GFAP), marking the vasculature overlaying the nerve fiber layer (asterisk) and activated Müller glia (arrowheads in *Nfia/b* and *Nfia/b/x* conditional mutants). (B) Expression of beta-catenin (*Ctnnb1*) in P14 retinas marks the localization of tight junctions. Loss and disruption of b-catenin expression within the OLM (arrowheads) is indicative of Müller glial cell loss. (C) Resident or activated microglia are marker by *Iba1* expression in P14 retinas. (D) Quantification of the number of TUNEL-positive (Left) Amacrine cells, (Middle) Photoreceptors, or (Right) Bipolar cells within *Nfia/b/x* triple mutants or heterozygous controls. (E) Quantification of the total number of TUNEL-positive cells observed within images of *Nfia/b/x* triple mutant retinas. Numbers of TUNEL-positive cells co-labeled with cell type markers are shown. (F) Quantification of the distance from the outermost edge of inner plexiform layer (IPL) to the outer limiting membrane (OLM) or edge of the nuclear layer when no OLM is observed. Inset diagrams show representations of how measurements were performed.  $p < 0.0001$ . (G) Quantification of the number of microglia present per P14 retinal section in control and NFI transcription factor conditional mutants retinas.  $p < 0.0001$ . (H) Quantification of the number of proliferative cells within images of P28 retinas. An EdU pulse was given at P21 and chased until P28. P28 retinas were stained with proliferative cell marker *Mki67*. (I) Quantification of the percentage of EdU positive cells that co-labeled with either *Mki67* or Recoverin in *Nfia/b/x* triple mutant retinas. Statistics are the results of an unpaired t-test (D) or a one-way ANOVA followed by Tukey's multiple comparisons tests (F and G). Significant results of multiple comparisons tests are indicated as \* -  $p < 0.05$  \*\* -  $p < 0.01$ , \*\*\* -  $p < 0.001$ , and \*\*\*\* -  $p < 0.0001$  in panels F and G. Statistics in panel H represent results of unpaired t-test, \*\*\*\* -  $p < 0.0001$ . Data are presented as mean  $\pm$

SEM.  $n \geq 3$  animals per condition with 3 or more images quantified/animal. For distance measurements in (F), 3 measurements per retinal section were averaged per animal to account for potential section plane and localization (central to peripheral retina) differences that could affect distance metrics. Scale bars - 100 $\mu$ m. Abbreviations: RGCL - Retinal Ganglion Cell Layer

**Supplementary Figure 20. Nfi mutant and control scRNA-seq - Related to Figure 7.** (A) QC metrics of scRNA-seq datasets analyzing Nfia/b/x triple mutant and heterozygous control retinas at P14, including (bottom) numbers of annotated retinal cell types within each sample. (B) Boxplot displaying the total number of expressed genes across the genotypes. (C) Boxplot displaying the total number of transcripts detected within cells across each sample. (D-E) Initial UMAP dimension reduction of the scRNA-seq datasets colored by (D) sample and (E) annotated cell type. (F) UMAP dimension reduction of the reduced retina dataset, colored by sample. Abbreviations: Photo. Precurs. - Photoreceptor Precursors; RGCs - Retinal Ganglion Cells.

### Supplemental Tables

**Table S1** - Smart-Seq2 high variance genes. Related to Figure 1B-D.

**Table S2** - Smart-Seq2 differential gene test - RPCs. Related to Figure 1B-D.

**Table S3** - Smart-Seq2 differential gene test - All cell types. Related to Figure 1B-D.

**Table S4** - High variance genes used for UMAP dimension reduction on 10x samples. Related to Figure 1E-F and Figure S2F-I.

**Table S5** - 10x cell type features. Related to Figure 1E-G and Figure S2J-M.

**Table S6** - High variance genes across 10x retinal cells. Related to Figure 2.

**Table S7** - Genes displaying differential expression across retina pseudotime. Related to Figure 2D.

**Table S8** - Gene weights within scCoGAPS patterns. Related to Figure 4.

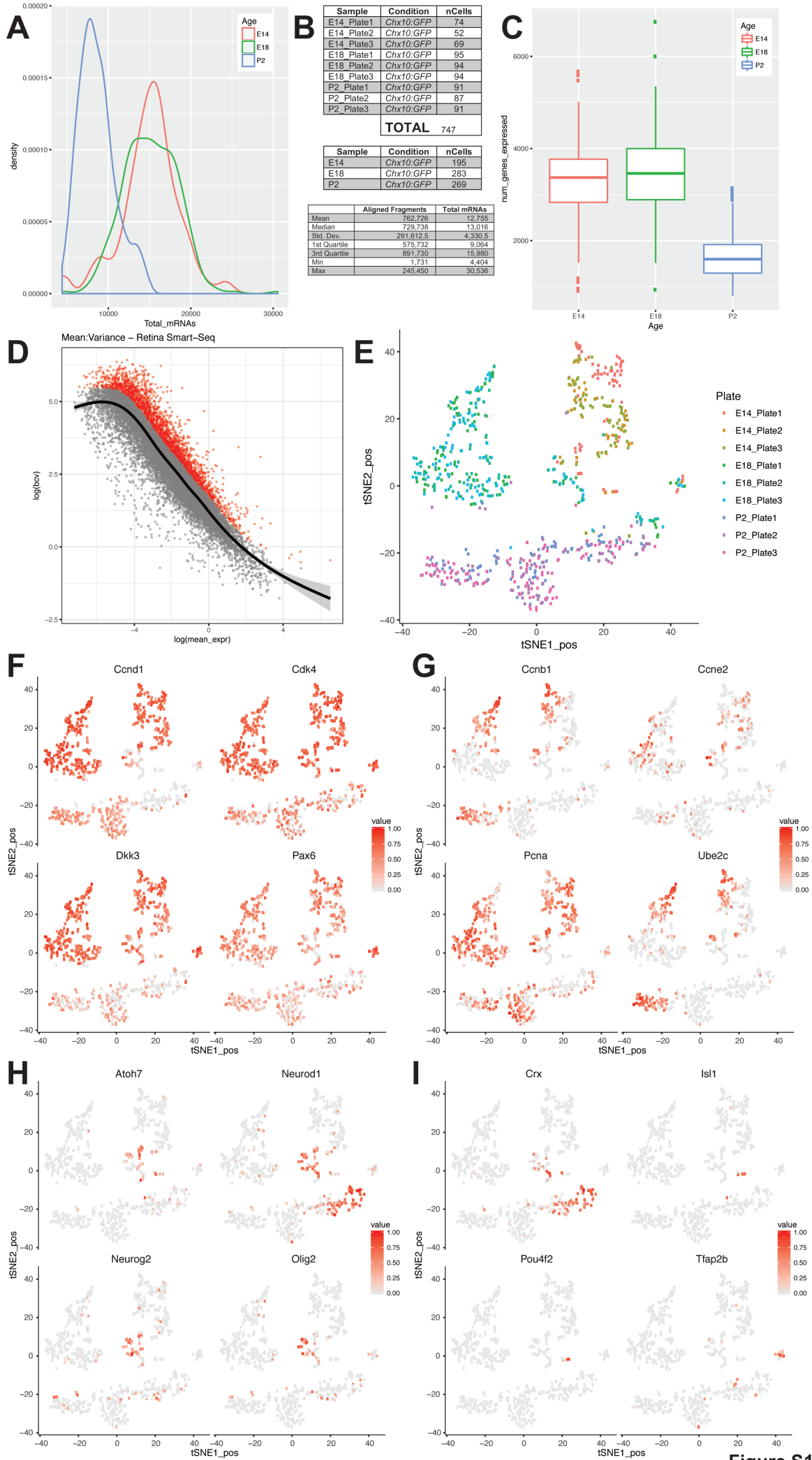


Figure S1

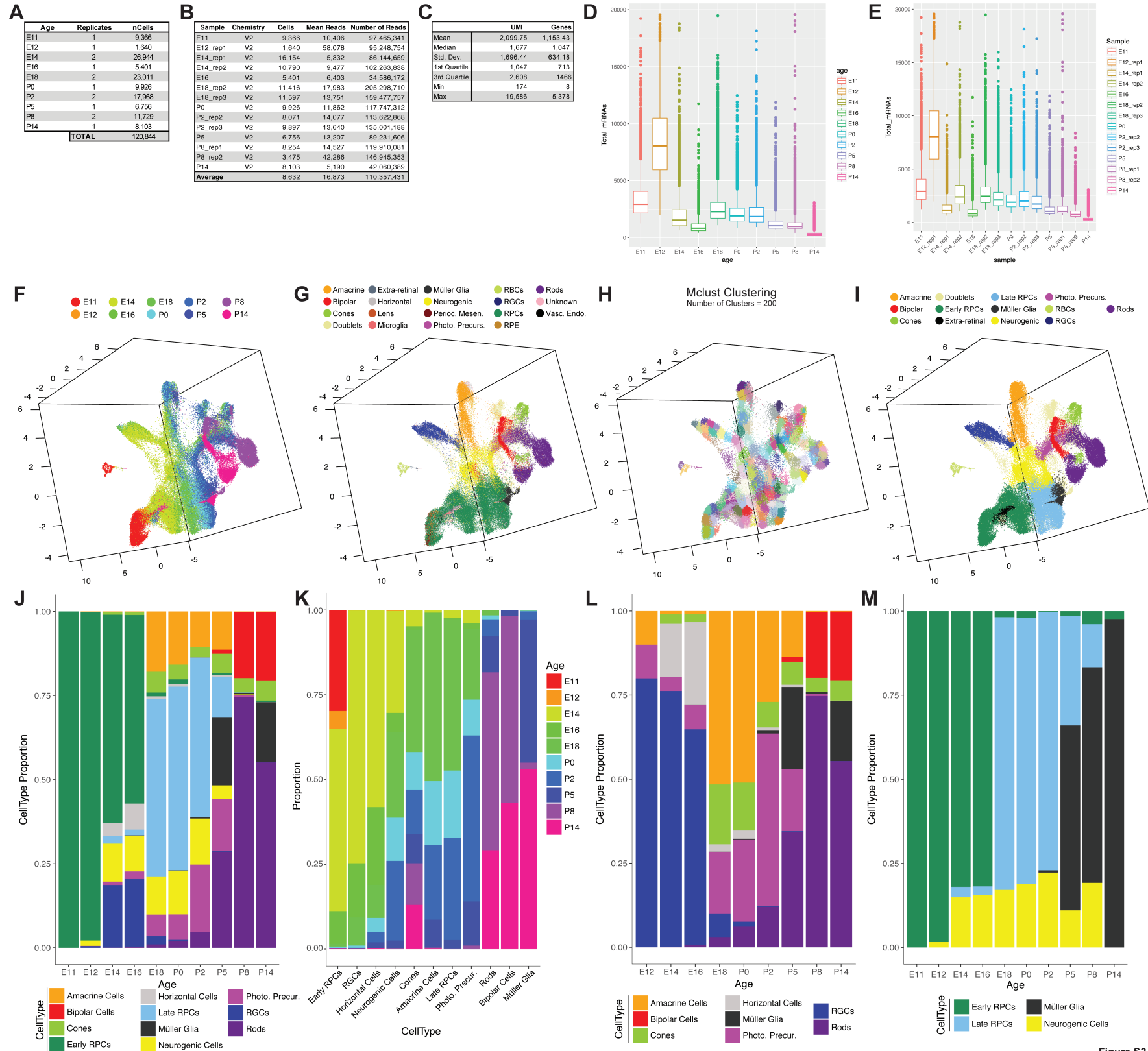
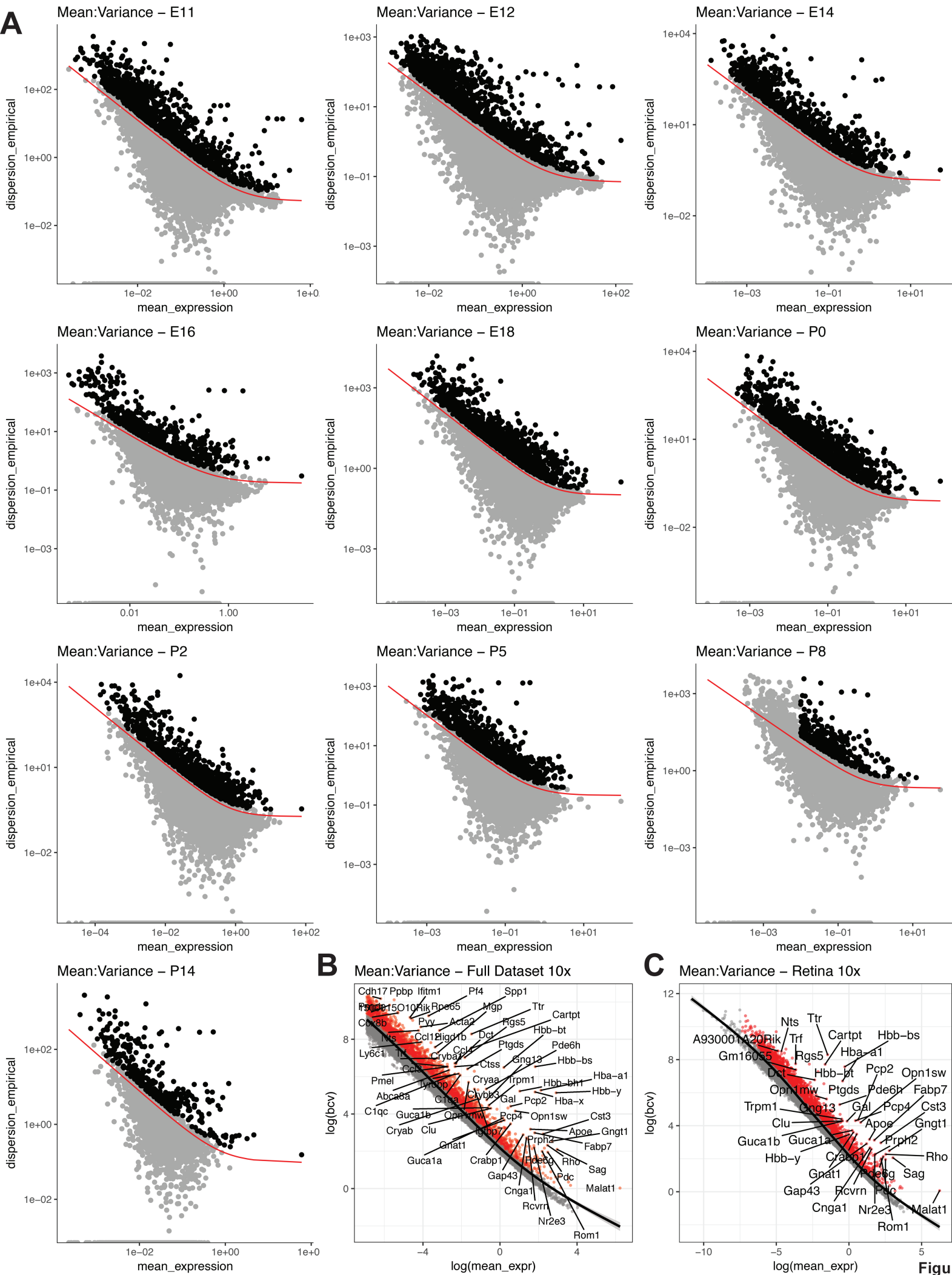


Figure S2





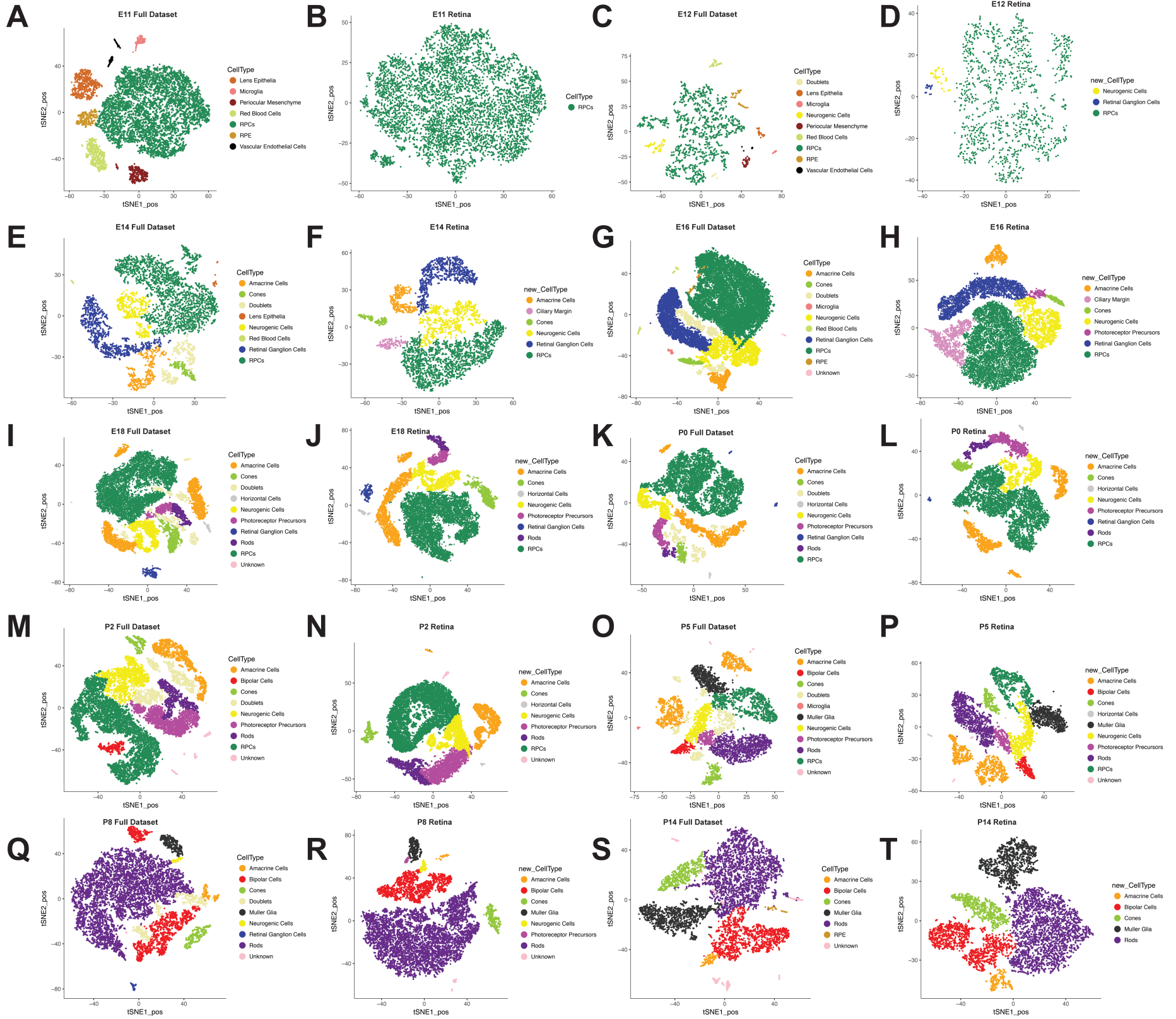


Figure S4

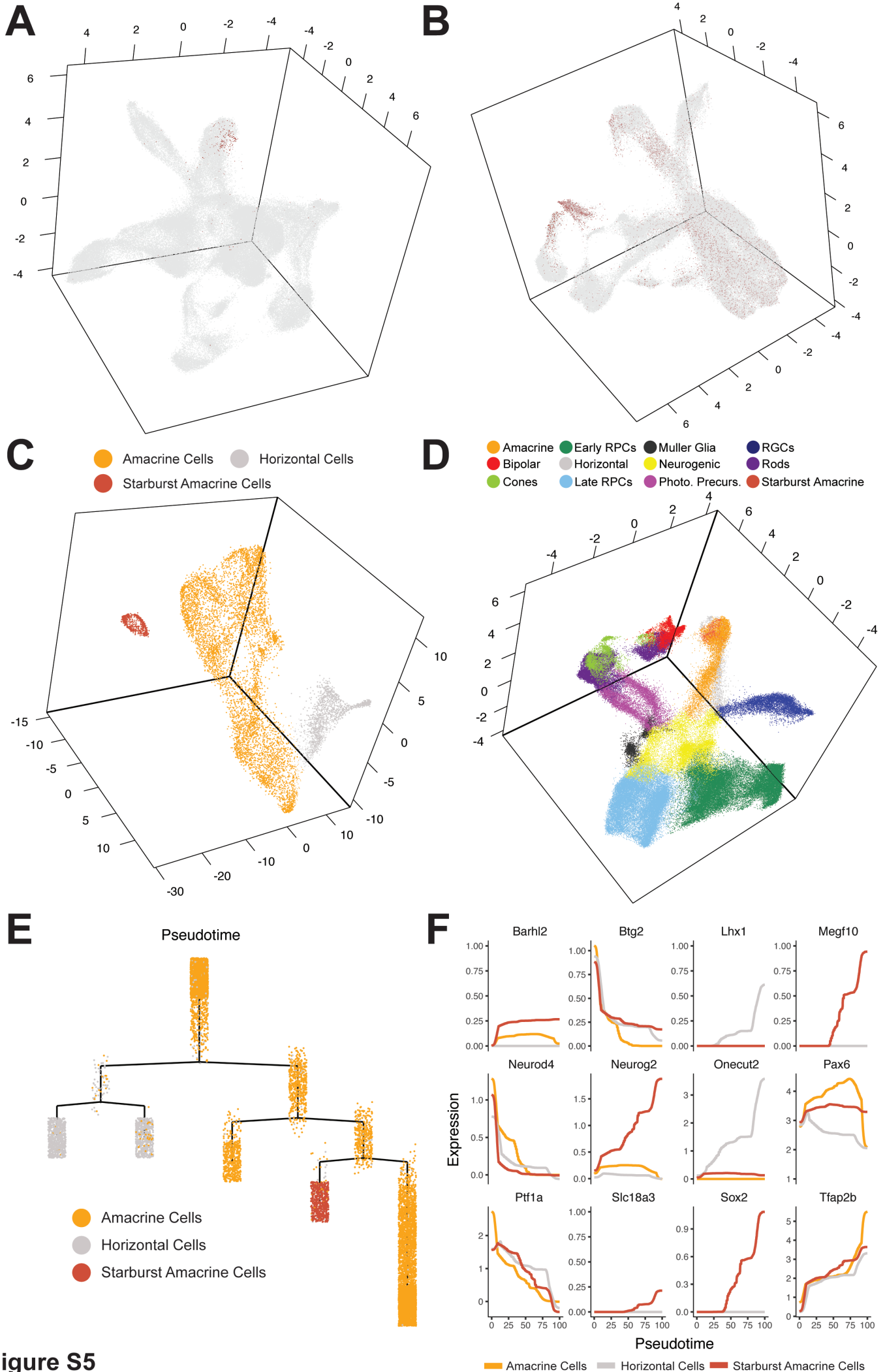


Figure S5

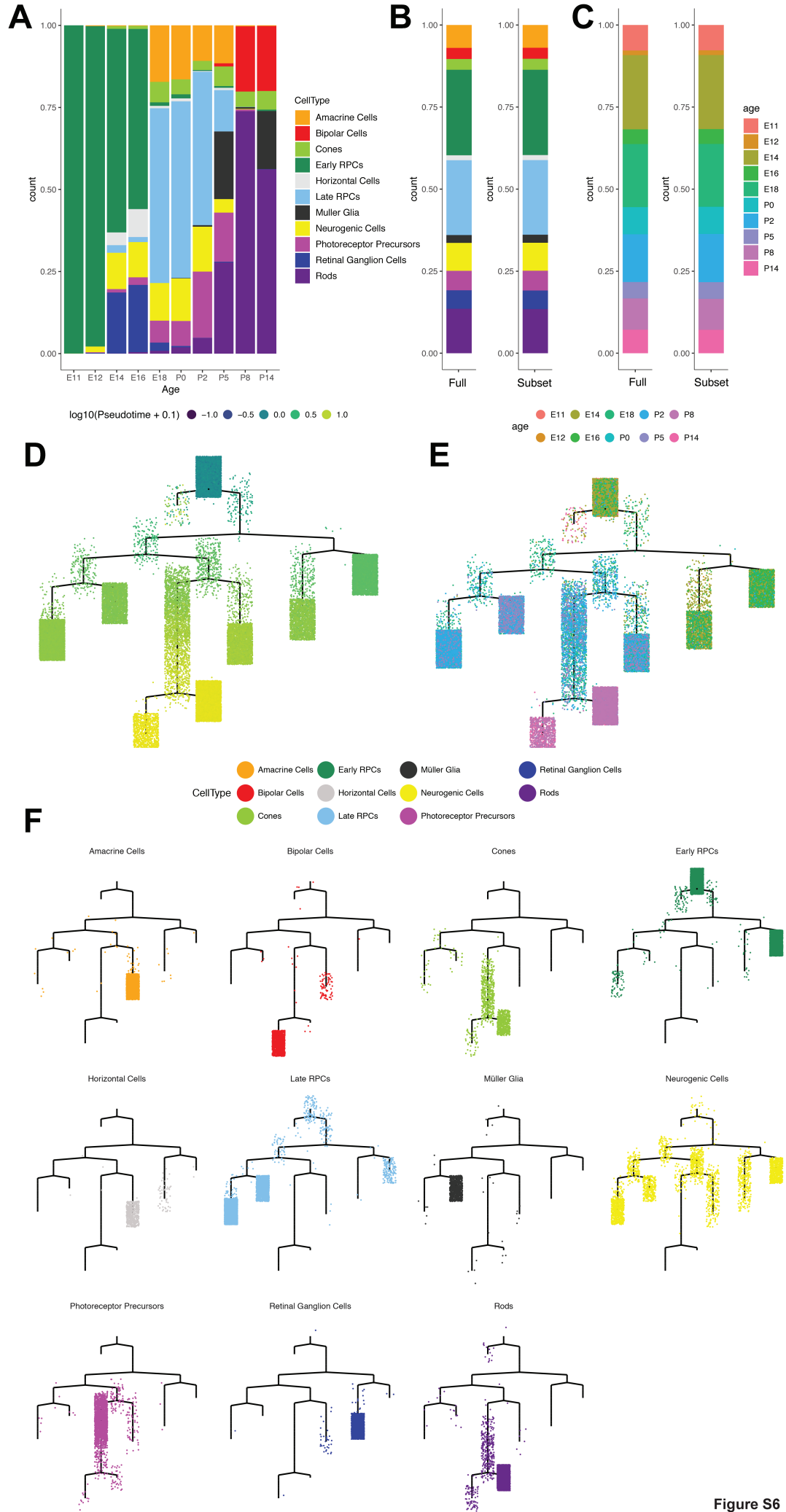


Figure S6

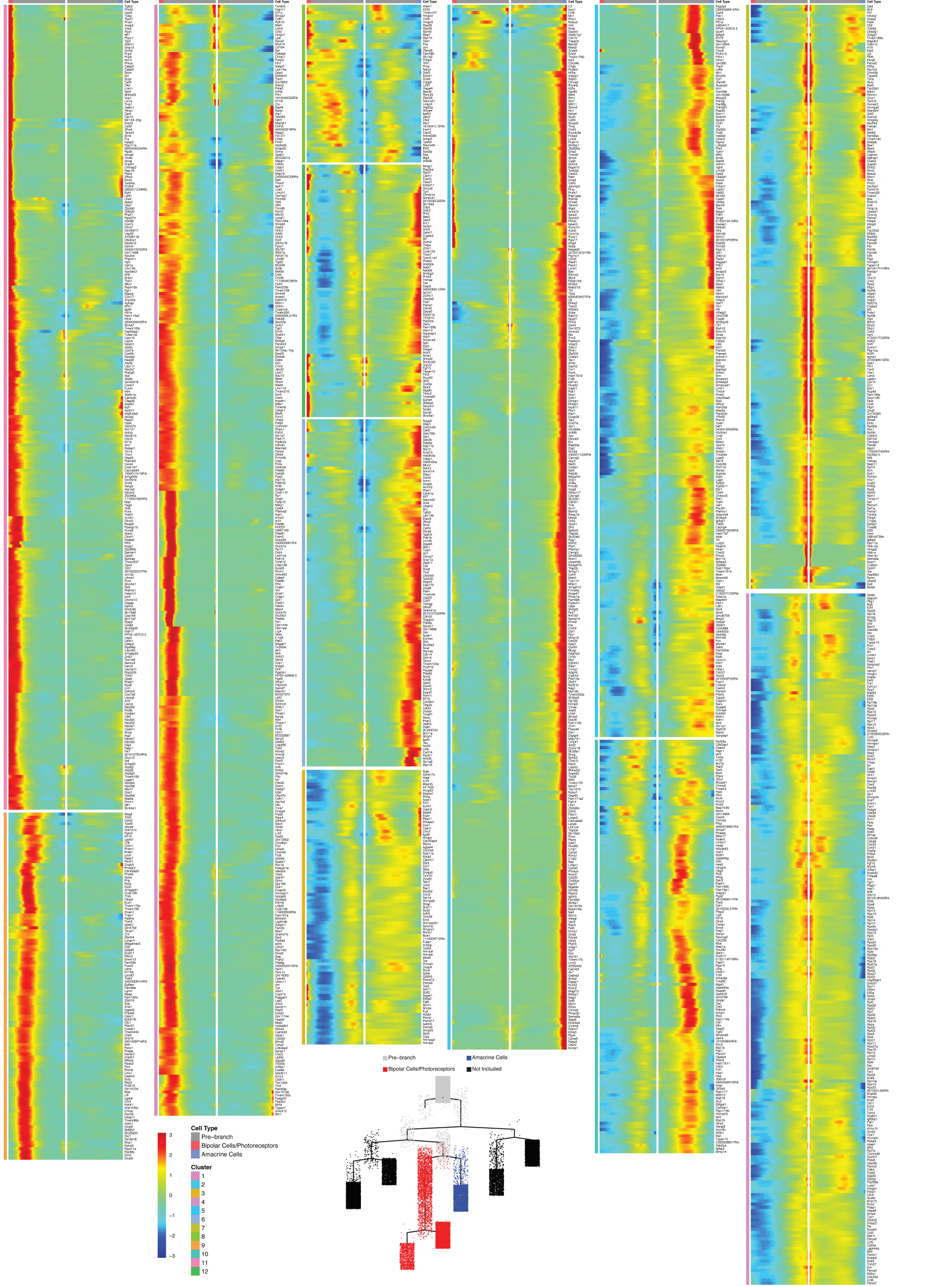


Figure S7

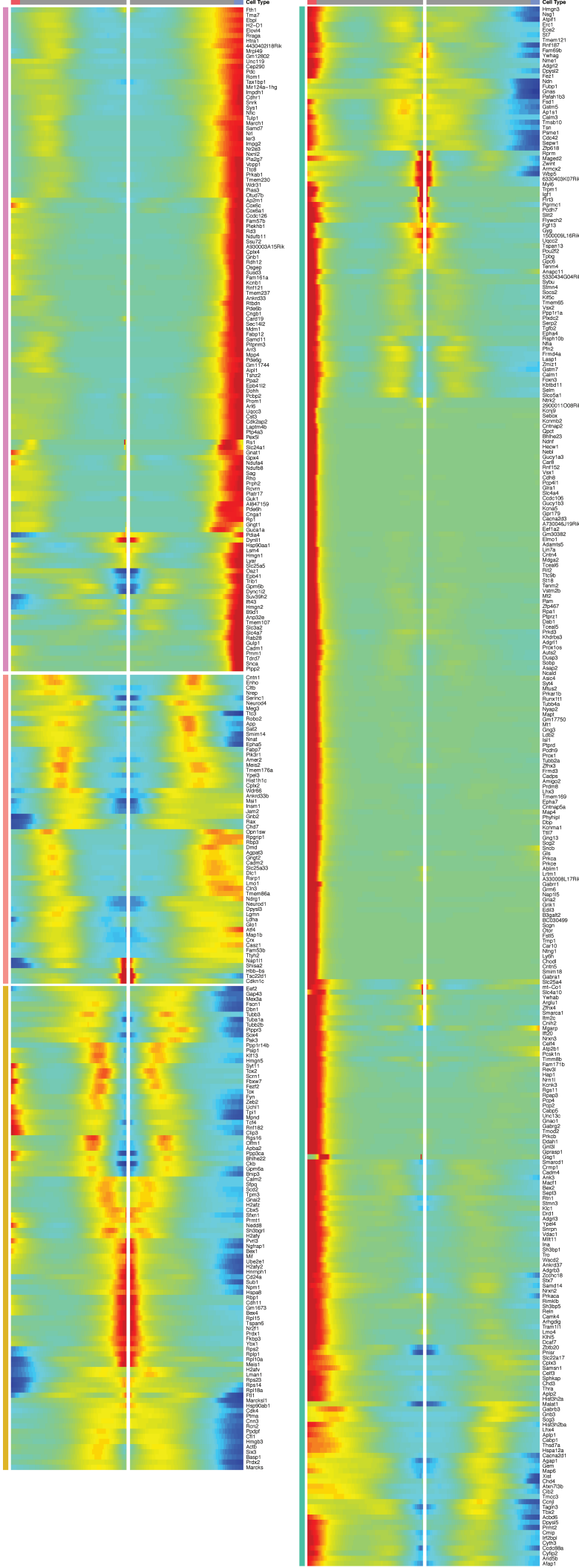


Figure S8

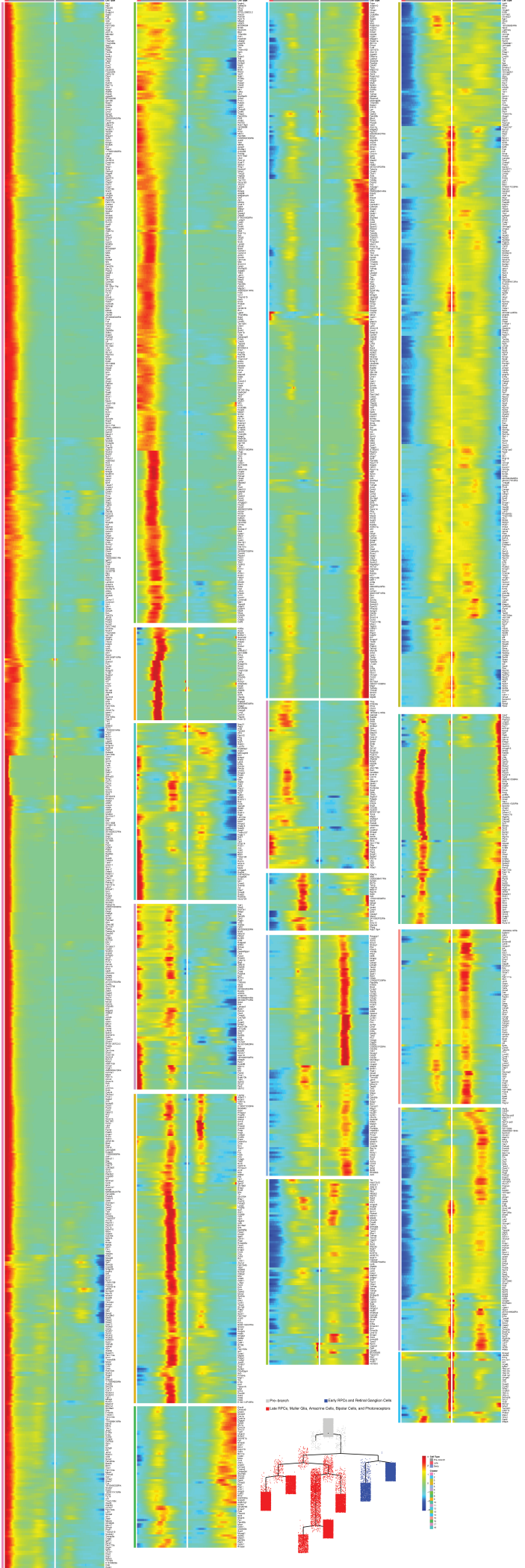


Figure S9

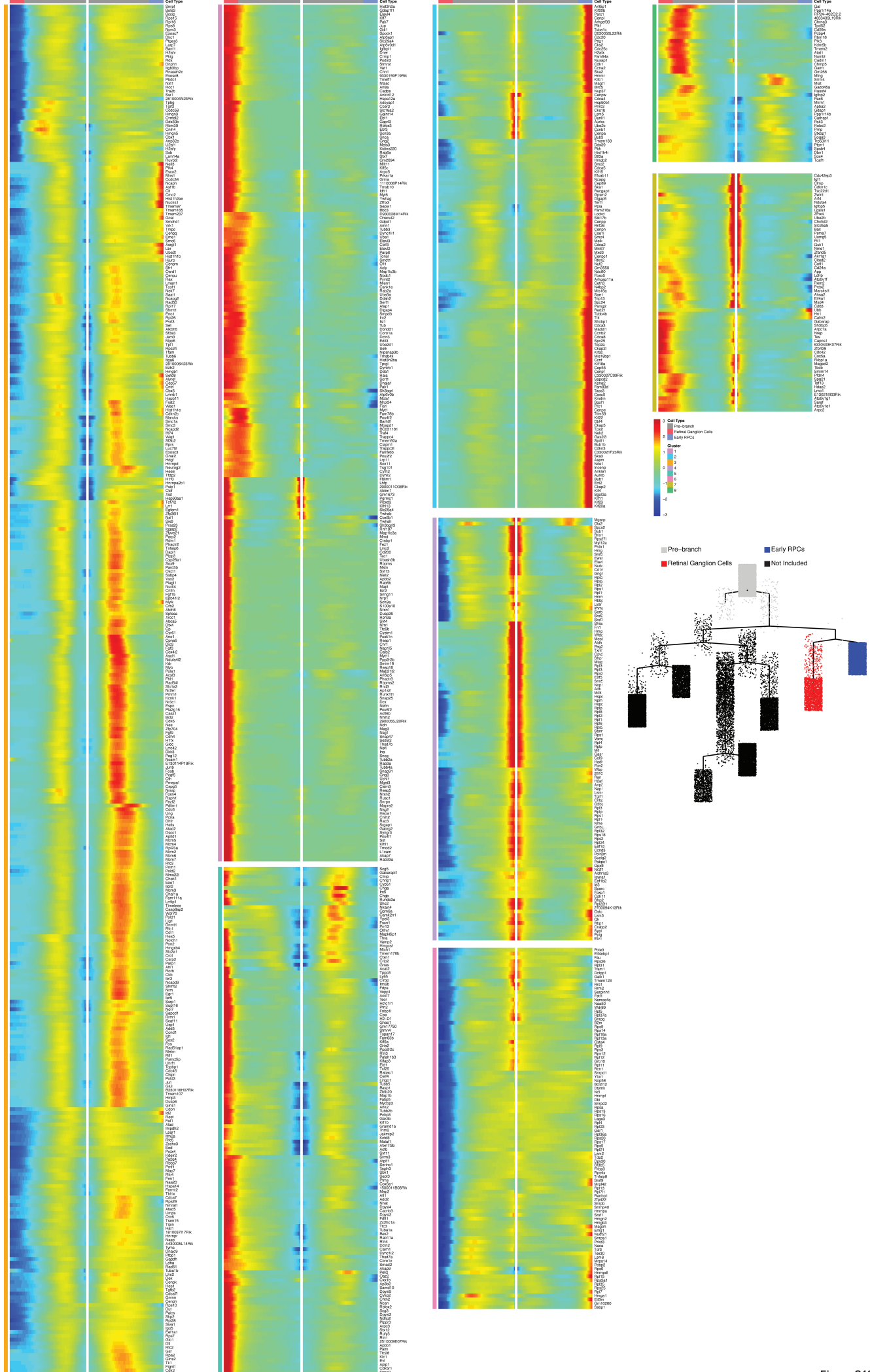


Figure S10



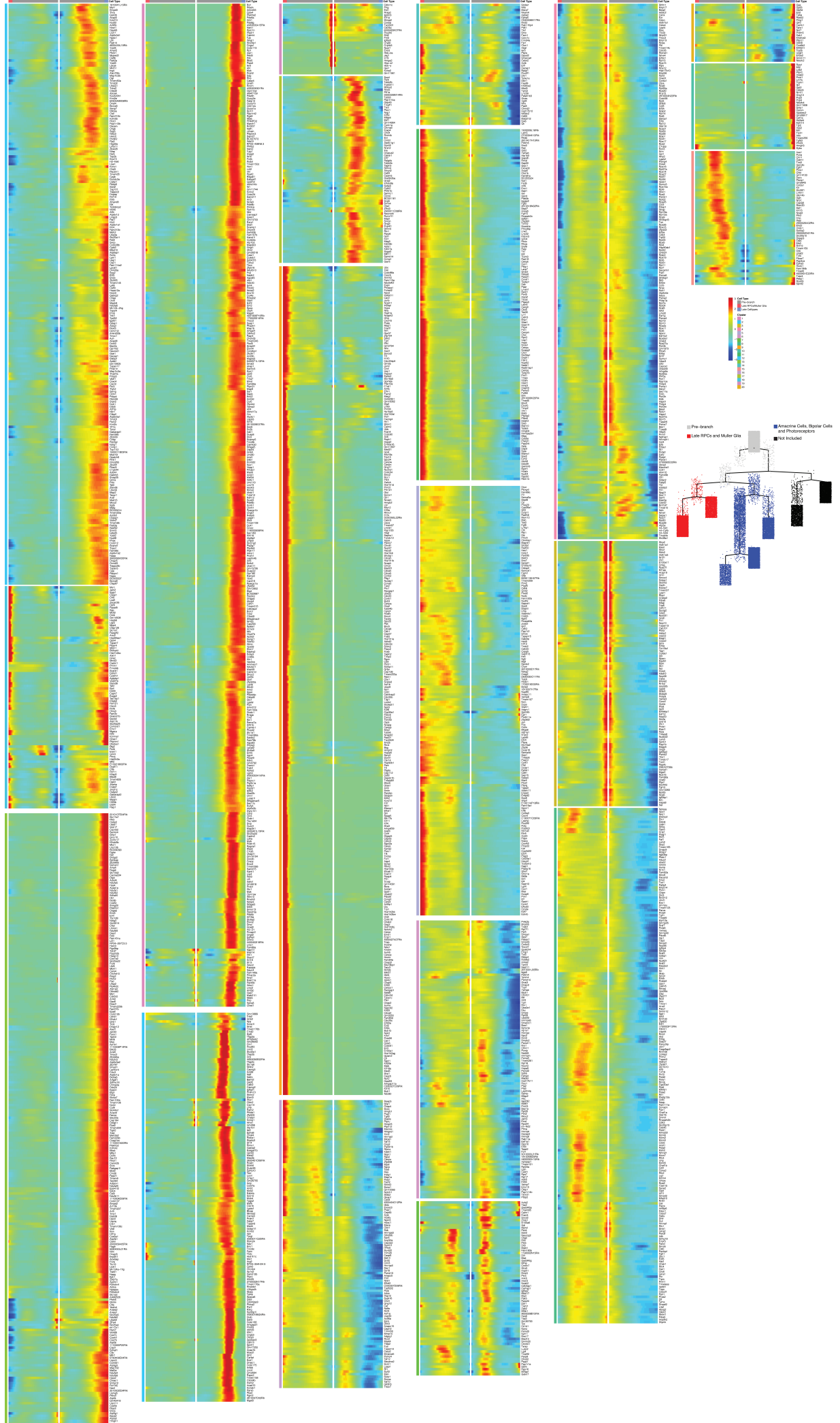


Figure S11

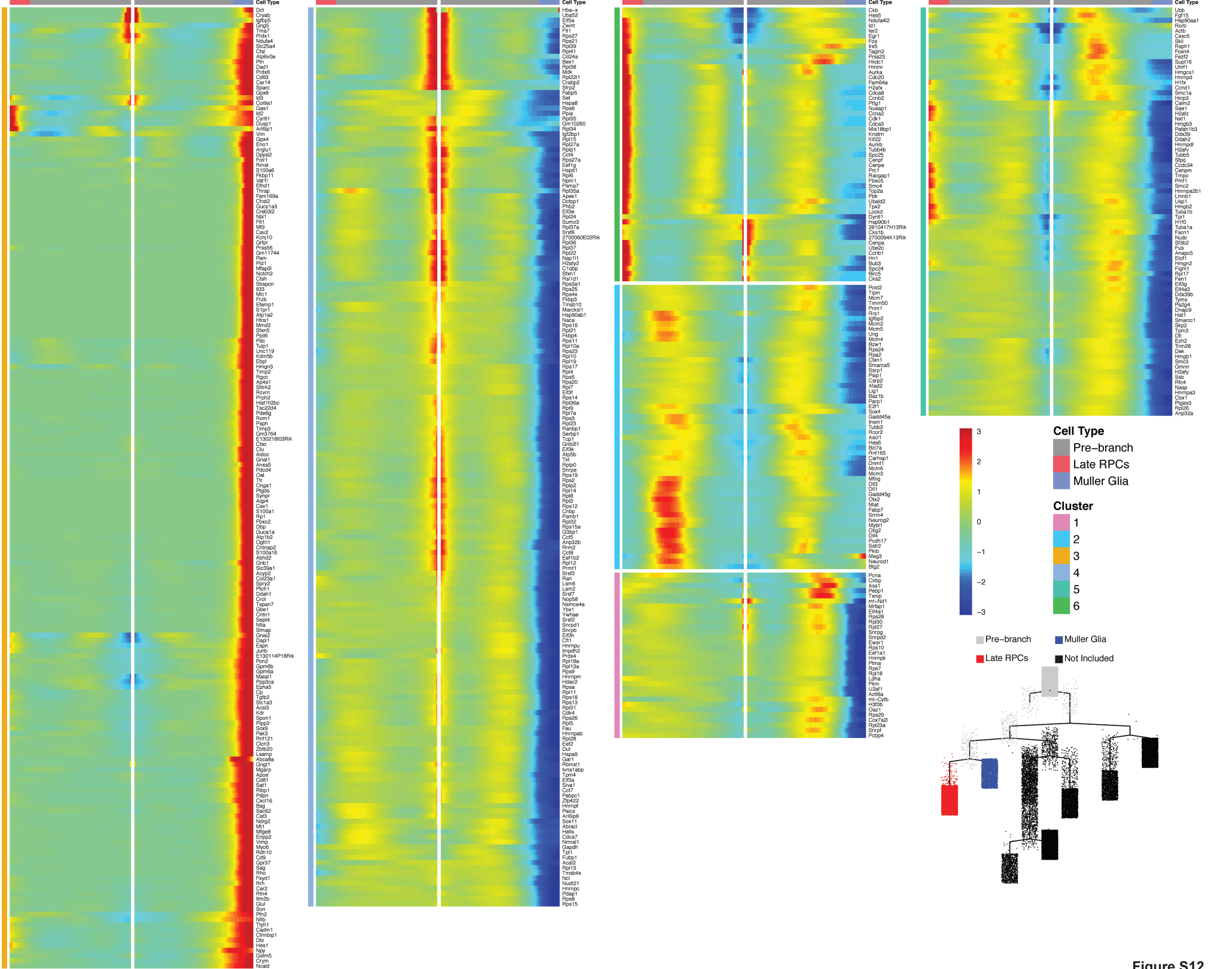


Figure S12

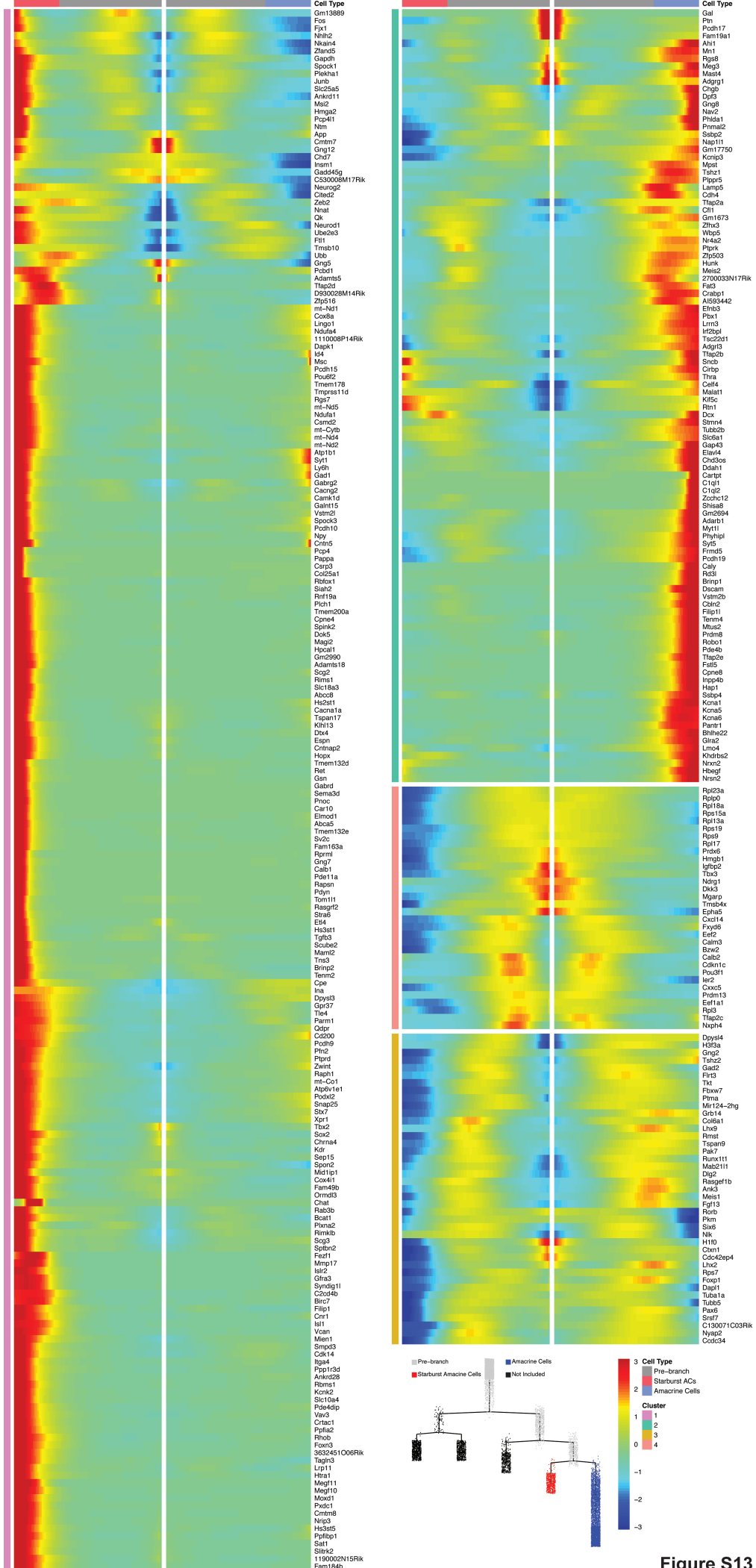


Figure S13

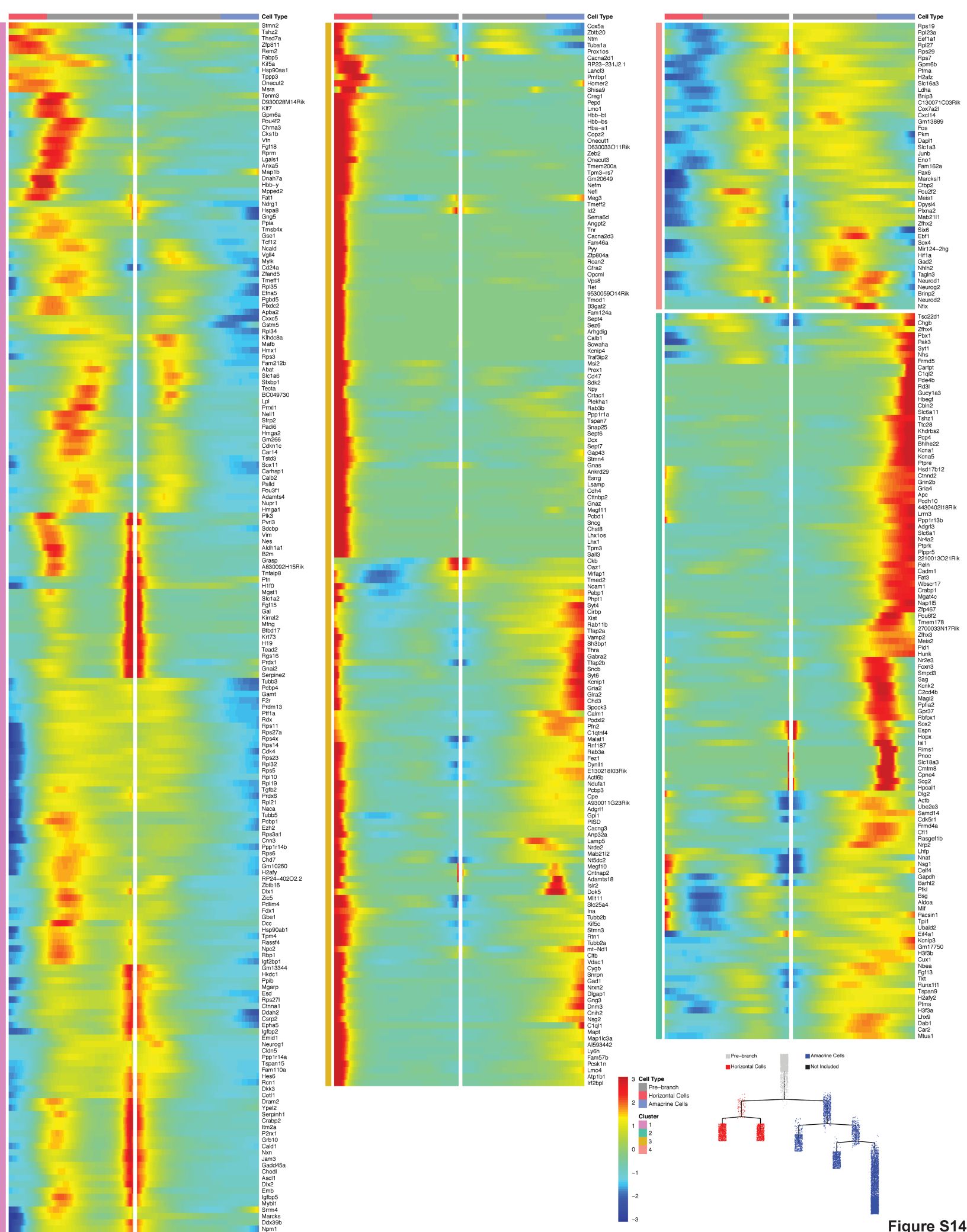


Figure S14

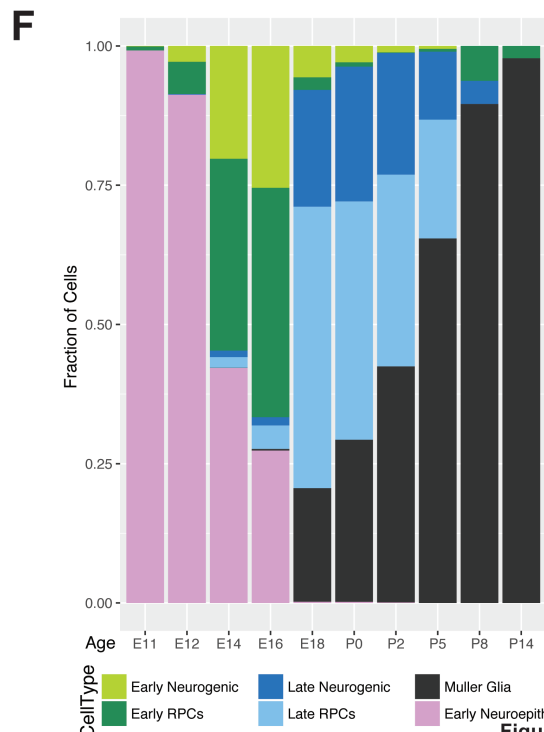
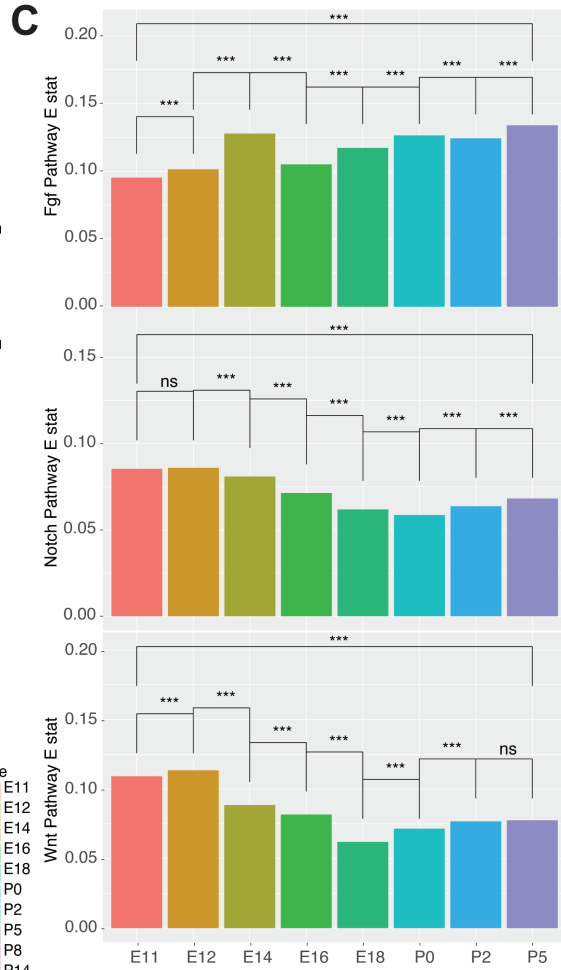
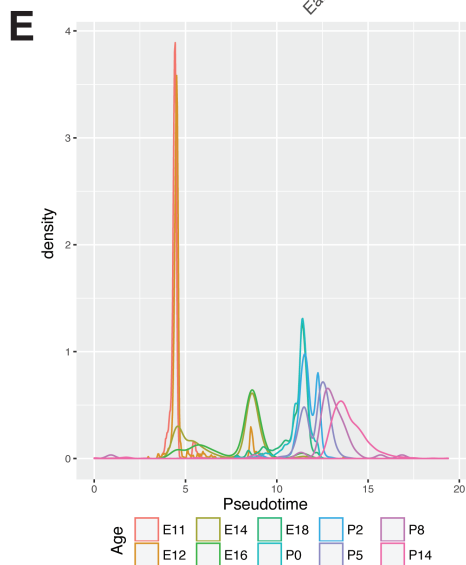
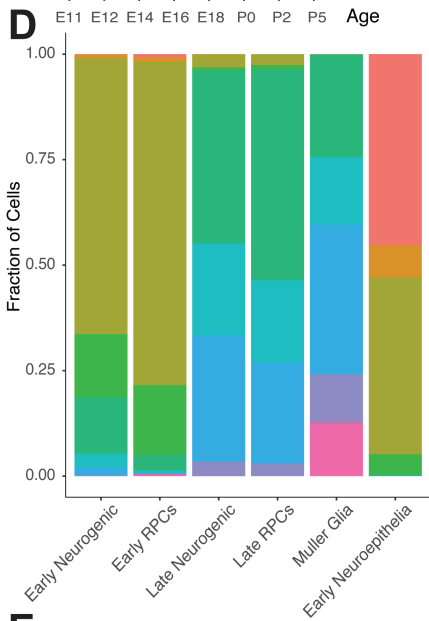
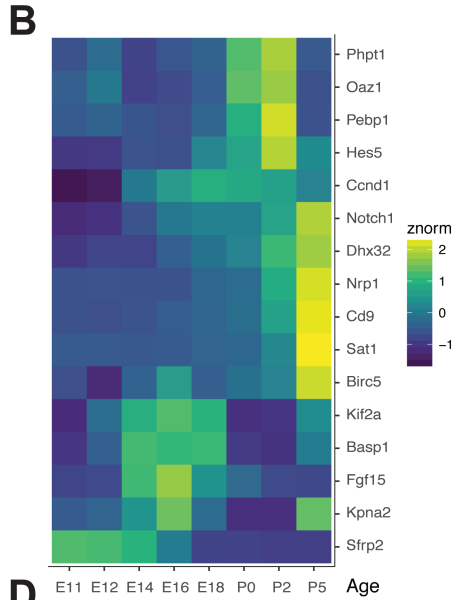
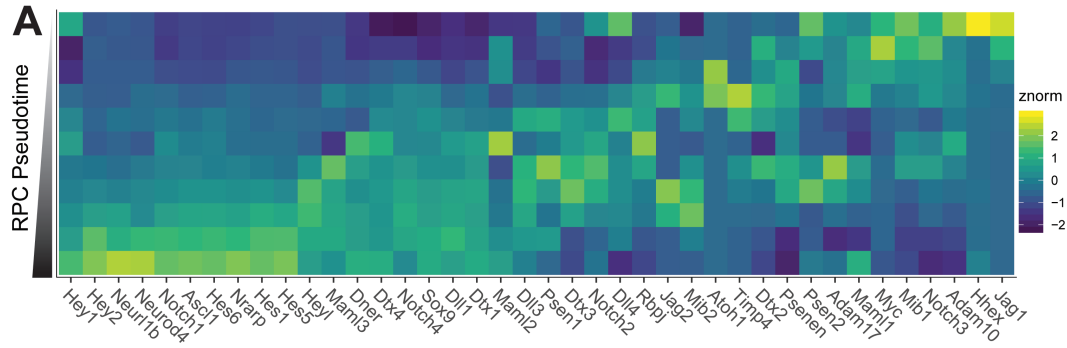
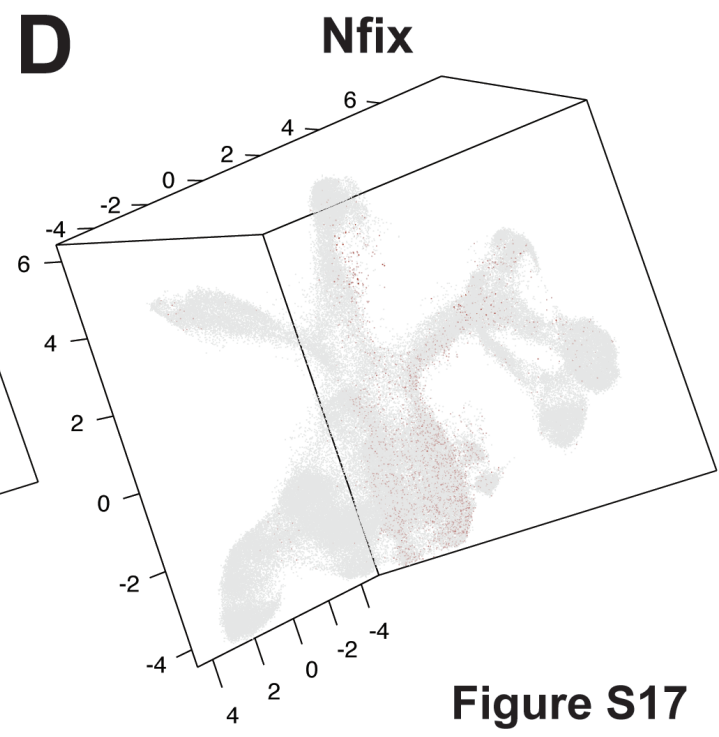
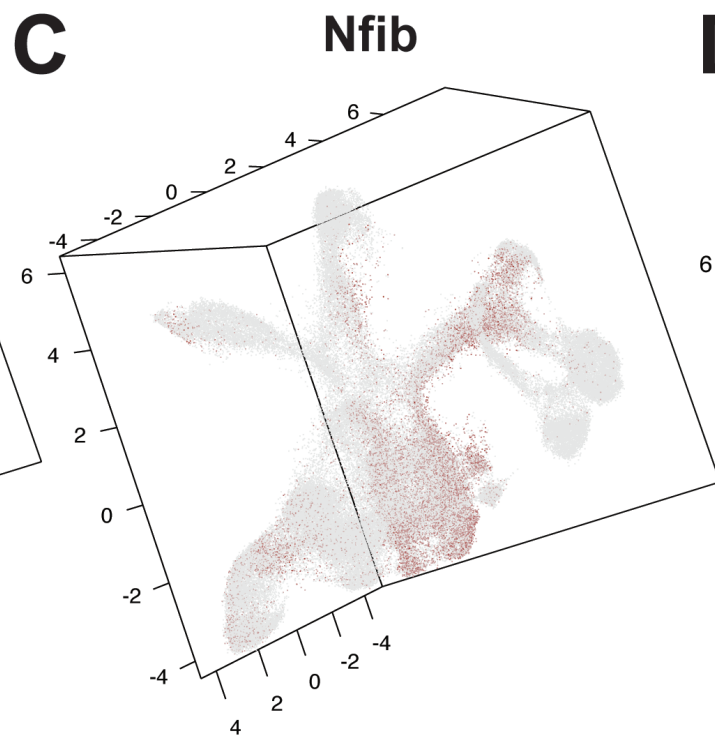
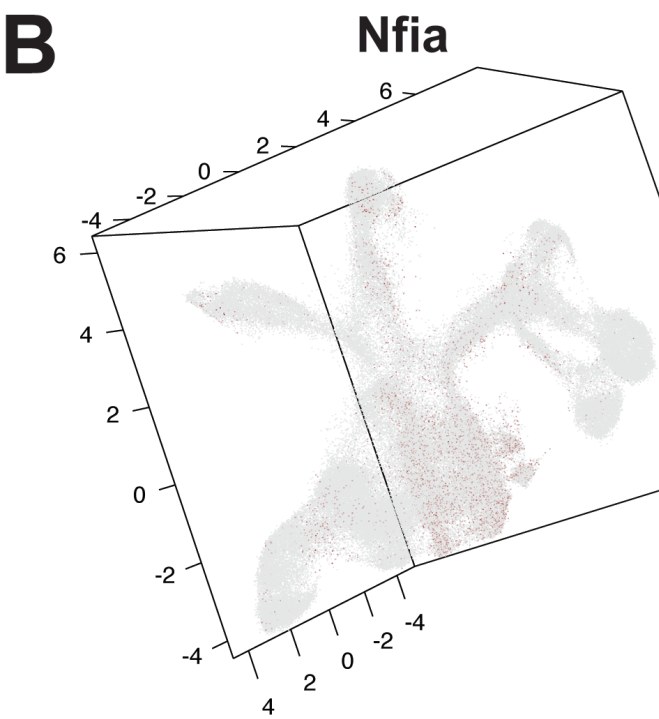
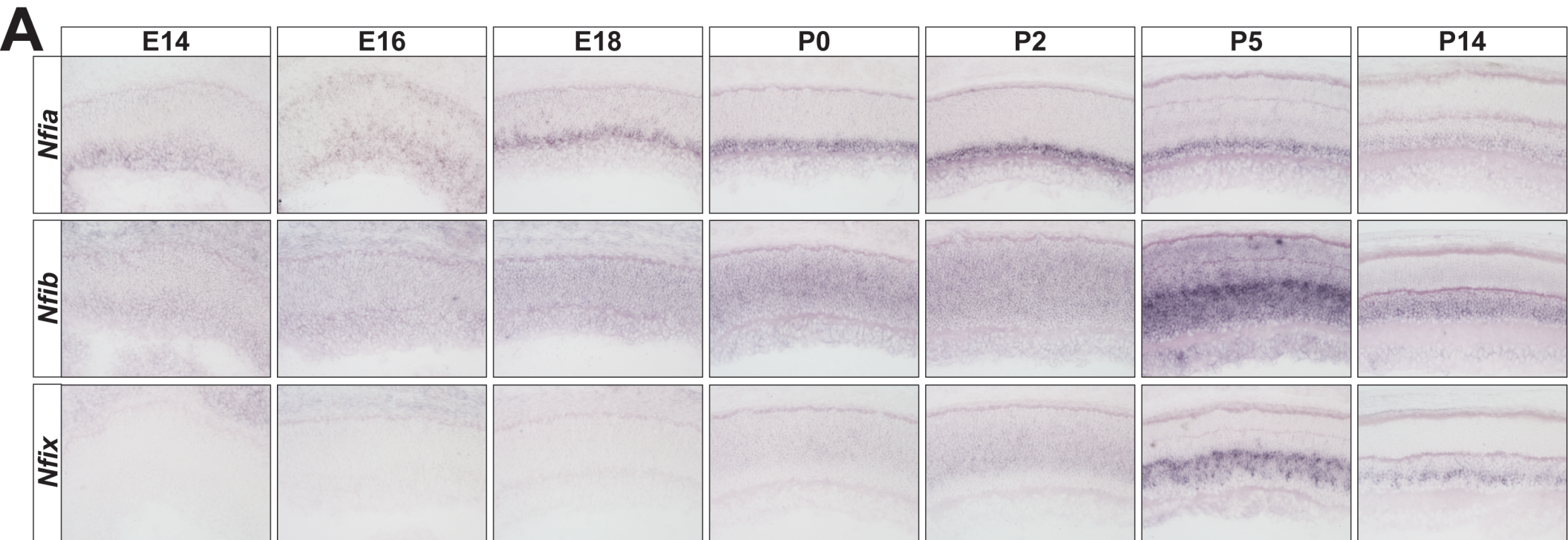


Figure S15



Figure S16



**Figure S17**

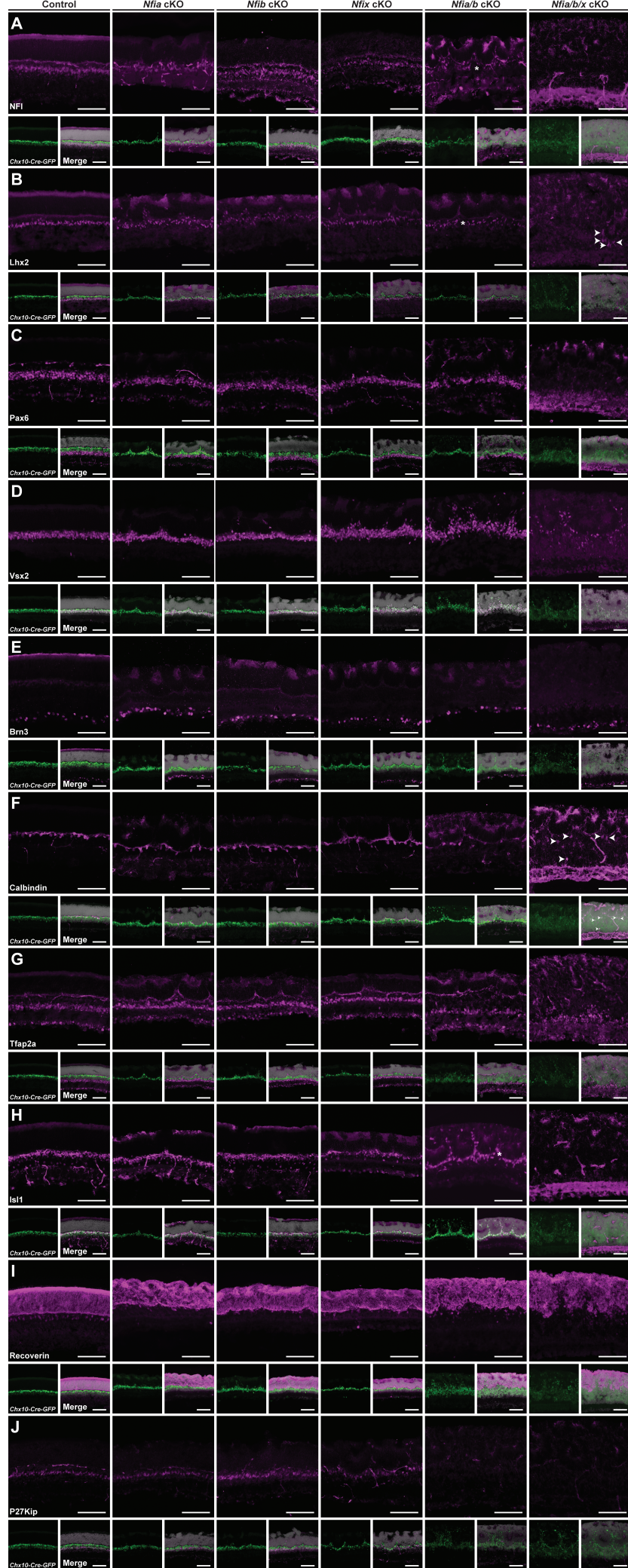
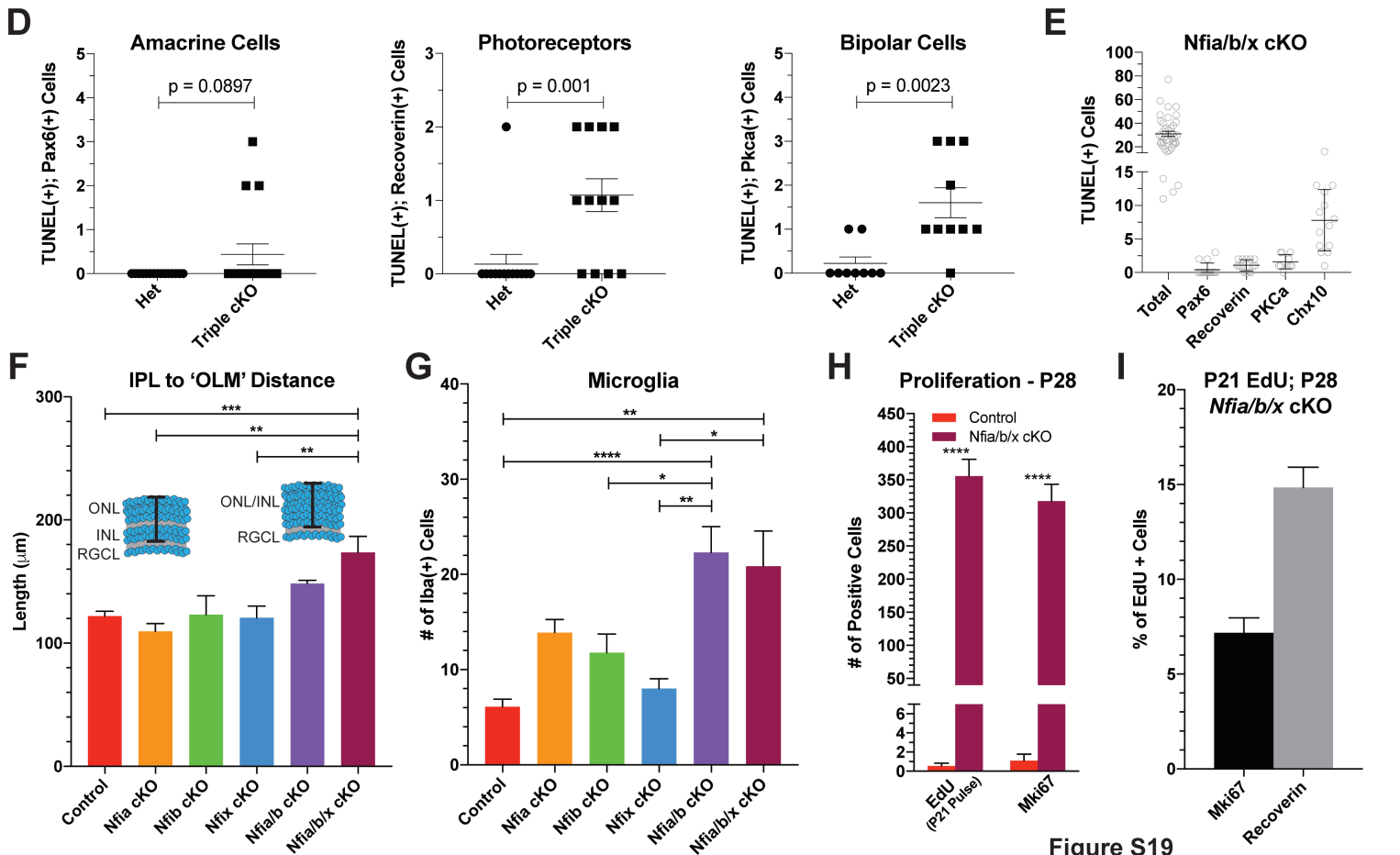
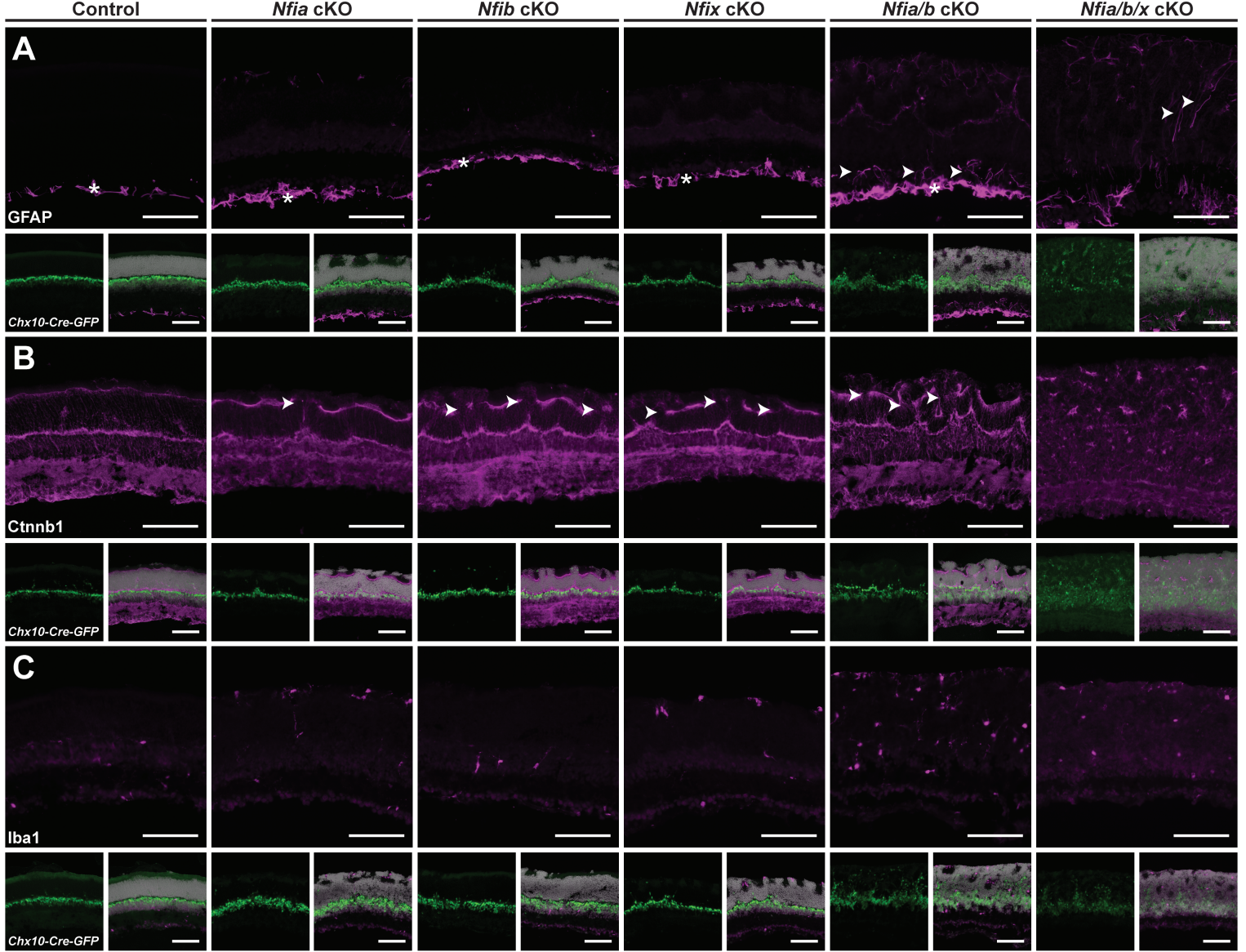


Figure S18





Sample	Age	# Cells (Initial)	Mean Reads	Number of Reads	# Cells (After Pre-Processing)
Nfia/b/x_Het_Rep1	P14	6,203	28,513	176,869,949	6,148
Nfia/b/x_Het_Rep2	P14	5,341	37,391	199,709,751	5,341
Nfia/b/x_tCKO_Rep1	P14	9,388	16,732	157,083,612	9,378
Nfia/b/x_tCKO_Rep3	P14	5,950	28,604	170,194,565	5,670
<b>Average</b>		6,721	27,810	175,964,469	6,634
<b>Total</b>		26,882			26,537

	Mean	Median	Std. Dev	1st Quartile	3rd Quartile	Min	Max
<b>UMI</b>	3786	2877	3113.64	1858	4613	546	19957
<b>Genes</b>	1686	1509	916.70	1063	2112	49	5605

	Amacrine	Bipolar	Cone	Horizontal	Muller Glia	Neurogenic	Photo Precurs	RGC	Rod	RPC
Nfia/b/x_Het_Rep1	1777	1614	356	93	538	23	53	102	539	28
Nfia/b/x_Het_Rep2	610	873	467	25	267	51	524	47	1993	62
Nfia/b/x_tCKO_Rep1	1472	128	709	25	10	1813	1233	93	333	2607
Nfia/b/x_tCKO_Rep3	412	15	282	17	7	1332	885	25	145	1681

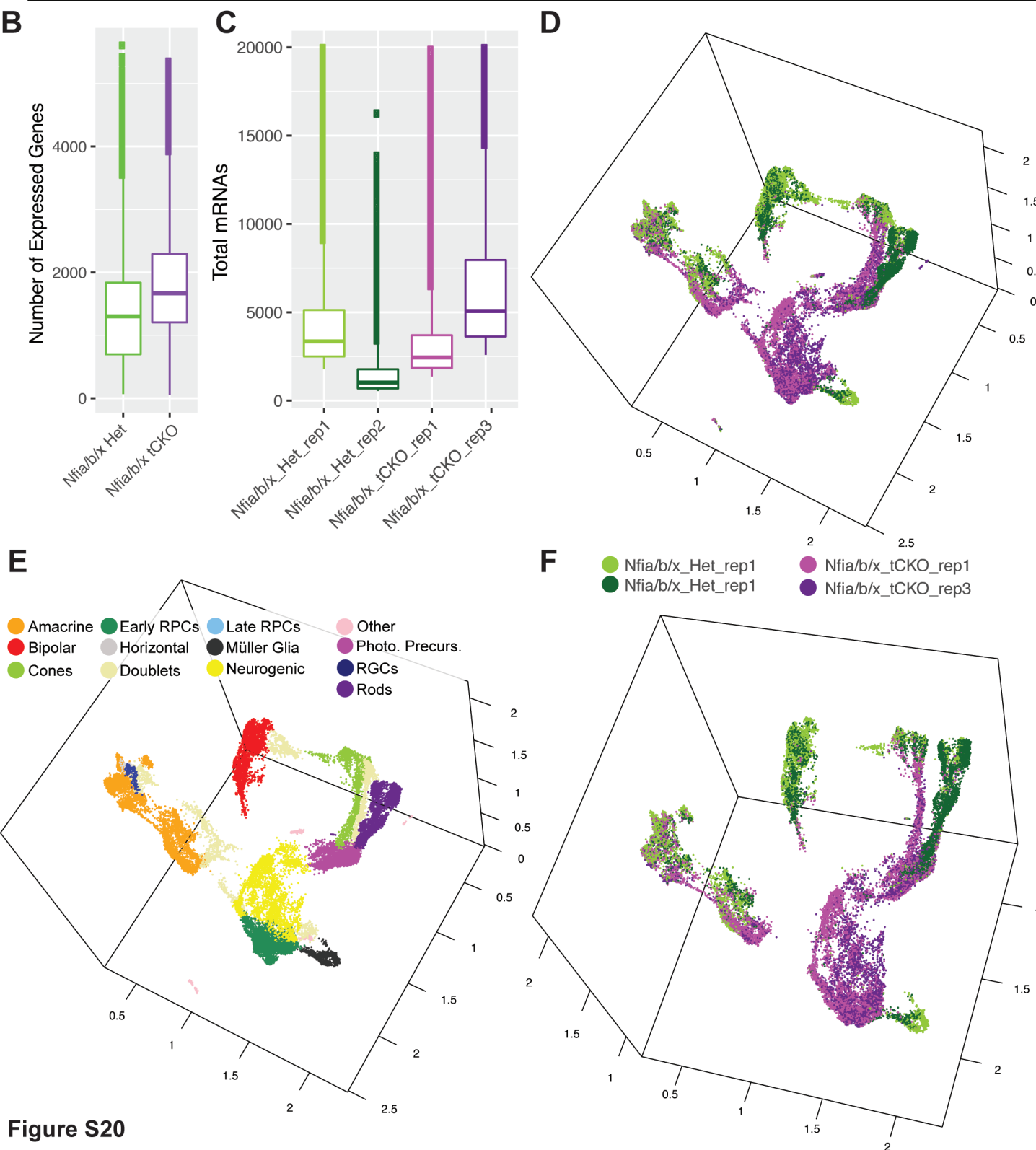


Figure S20